Journal of Power Sources 192 (2009) 21–26

Contents lists available at ScienceDirect

Journal of Power Sources

journal homepage: www.elsevier.com/locate/jpowsour

In situ generation of hydrogen from water by aluminum corrosion in solutions of sodium aluminate

Lluís Soler[a], Angélica María Candela[a], Jorge Macanás[b], Maria Muñoz[a,*], Juan Casado[a]

[a] *Centre Grup de Tècniques de Separació en Química (GTS), Unitat de Química Analítica, Departament de Química, Universitat Autònoma de Barcelona, Campus UAB s/n, 08193 Bellaterra, Barcelona, Catalonia, Spain*
[b] *Laboratoire de Génie Chimique, UMR 5503 CNRS-INPT-UPS, Université de Toulouse, Toulouse, France*

ARTICLE INFO

Article history:
Received 13 October 2008
Received in revised form 5 November 2008
Accepted 5 November 2008
Available online 13 November 2008

Keywords:
Hydrogen generation
Aluminum corrosion
Sodium aluminate

ABSTRACT

A new process to obtain hydrogen from water using aluminum in sodium aluminate solutions is described and compared with results obtained in aqueous sodium hydroxide. This process consumes only water and aluminum, which are raw materials much cheaper than other compounds used for *in situ* hydrogen generation, such as hydrocarbons and chemical hydrides, respectively. As a consequence, our process could be an economically feasible alternative for hydrogen to supply fuel cells. Results showed an improvement of the maximum rates and yields of hydrogen production when $NaAlO_2$ was used instead of NaOH in aqueous solutions. Yields of 100% have been reached using $NaAlO_2$ concentrations higher than 0.65 M and first order kinetics at concentrations below 0.75 M has been confirmed. Two different heterogeneous kinetic models are verified for $NaAlO_2$ aqueous solutions. The activation energy (E_a) of the process with $NaAlO_2$ is 71 kJ mol^{-1}, confirming a control by a chemical step. A mechanism unifying the behavior of Al corrosion in NaOH and $NaAlO_2$ solutions is presented. The application of this process could reduce costs in power sources based on fuel cells that nowadays use hydrides as raw material for hydrogen production.

1. Introduction

There is an urgent demand to implement renewable and clean fuel alternatives to satisfy the energetic demand of the 21st century due to fossil fuel depletion and to the importance of reducing emissions of greenhouse and polluting gases, responsible of harmful effects like the climate change. Hydrogen is a non-polluting fuel and a clean energy vector that can be consumed in a fuel cell, converting chemical into electrical energy with high performance in mild conditions. Fuel cells are attractive devices for many types of stationary and mobile applications, such as electric vehicles and portable electronic devices, due to their high energy densities [1]. However, the development of effective methods for hydrogen production and storage are an indispensable requisite to fulfill these expectations [2,3].

Hydrogen generation from reaction of chemical hydrides in aqueous solutions has reduced hydrogen storage volume and/or weight in comparison to conventional systems such as high pressure or cryogenic storage [4]. Among these chemicals, sodium borohydride ($NaBH_4$) has been proved to be safe and able to reach a gravimetric hydrogen capacity of 21.3%. The hydrolysis reaction of sodium borohydride can be significantly accelerated by addition of acids or certain metal salts with catalytic effect. Nevertheless, sodium borohydride has some disadvantages: it is unstable and sensitive to moisture in the air and it is an expensive raw material (55 \$ kg^{-1}) [5] as compared to current fossil fuels prices, which are nowadays the most used raw materials in hydrogen production.

On the other hand, among the different metals that can react with aqueous solutions to generate hydrogen, aluminum and its alloys have been recognized among the most suitable materials for the development of future processes of hydrogen production [6]. Aluminum can be stored and transported in a much simpler, safer and cheaper way than hydrogen. It is stable under usual conditions and much less expensive than sodium borohydride: the price of aluminum powder (3 \$ kg^{-1}) is 10–20 times lower than the price of sodium borohydride [7,8].

The reactions of aluminum with aqueous solutions of sodium hydroxide have been previously studied [9–12]:

$$2Al + 6H_2O + 2NaOH \rightarrow 2NaAl(OH)_4 + 3H_2 \quad (1)$$

$$NaAl(OH)_4 \rightarrow NaOH + Al(OH)_3 \quad (2)$$

$$2Al + 6H_2O \rightarrow 2Al(OH)_3 + 3H_2 \quad (3)$$

Initially, the hydrogen generation reaction (1) consumes sodium hydroxide, but when the aluminate concentration exceeds the saturation limit, aluminate undergoes a decomposition reaction (2) that produces a crystalline precipitate of aluminum hydroxide with the

* Corresponding author at: Edifici C – Campus de la UAB s/n, 08193 Bellaterra, Barcelona, Catalonia, Spain. Tel.: +34 93 581 2123; fax: +34 93 581 2379.
E-mail address: maria.munoz@uab.cat (M. Muñoz).

0378-7753/$ – see front matter © 2008 Elsevier B.V. All rights reserved.
doi:10.1016/j.jpowsour.2008.11.009

Nomenclature

A	constant pre-exponential factor (s^{-1})
b	stoichiometric factor
C_{NaAlO_2}	molar concentration of $NaAlO_2$ ($mol\,dm^{-3}$)
E_a	activation energy ($kJ\,mol^{-1}$)
k	rate constant (s^{-1})
k_{ex}	experimental rate constant for chemical step model (s^{-1})
k'_{ex}	experimental rate constant for mass transfer model (s^{-1})
k_q	chemical reaction rate constant ($m\,s^{-1}$)
n	order of reaction
r_0	initial radius of the Al reacting core (m)
R	ideal gas constant ($8.314\,J\,mol^{-1}\,K^{-1}$)
t	time (s)
T	temperature (K)
X	degree of reaction

Greek letters

ρ_{Al}	Al molar density ($mol\,dm^{-3}$)

regeneration of the alkali [9]. Reaction (2) has been studied in depth concerning the Al/air battery [13]. The overall hydrogen-generating reaction of aluminum in an aqueous solution is described by equation (3) [10,12,14]. This reaction has also been investigated in order to minimize the capacity loss and avoid the drop of Faradaic efficiency of Al anode [13]. Previous works [9–15] evidenced that the overall process should not consume alkali and it is able to produce hydrogen gas from Al with regeneration of hydroxyl ions. A major hurdle to the production of hydrogen via this corrosion reaction is that the aluminum surface is easily passivated [10], but the passivation can be minimized optimizing several experimental parameters such as temperature, alkali concentration, aluminum raw material form and solution composition.

Hydrogen generation systems based on Al corrosion do not need to be warmed up externally, since Al corrosion is an exothermic reaction. In addition, this reaction can be achieved under mild conditions of temperature and pressure, providing a stable and compact source of hydrogen, much less expensive than the hydrolysis of hydrides. Each kilogram of aluminum produces approximately 4 kWh of energy in the form of hydrogen [7] and, assuming an achievable 100% hydrogen generation efficiency, it is possible to reach a global gravimetric hydrogen capacity of 11.2% H_2, which is a significant value to accomplish the U.S. DOE research targets [16]. If needed, this gravimetric hydrogen capacity can be increased using a combination of Al and $NaBH_4$ to produce hydrogen [17].

One of the important commercial aluminum compounds is sodium aluminate, $NaAlO_2$. It is used in water treatment as an adjunct to water softening systems, as a coagulant aid to improve flocculation, and for the removal of dissolved silica and phosphates. Sodium aluminate has been known for many years as an intermediate product in the extraction and purification of gibbsite from bauxite ores by the Bayer Process [18]. Considerable research [19–21] has been devoted to determine the identity of soluble species in alkaline solutions of sodium aluminate (known as Bayer liquors) to provide a key to understanding critical aspects of this process, such as the unexpectedly slow precipitation and crystal growth kinetics of $Al(OH)_3$.

The main objective of this work is to demonstrate the feasibility of producing hydrogen by reaction of Al with aqueous solutions of sodium aluminate at mild temperatures. The basic idea is to take advantage of the alkaline properties of sodium aluminate to achieve a high pH and enhance the aluminum corrosion. The presence of sodium aluminate in the aqueous solution could reduce aluminum surface passivation, producing fuel cell grade hydrogen by a process that decreases overall hydrogen production costs. The effects of modifying several experimental parameters are reported in the present article and compared with our own results using NaOH solutions and with previous works.

2. Experimental

2.1. Chemicals

Sodium hydroxide (98% purity) was supplied by Panreac. Sodium aluminate anhydrous was supplied by Riedel-de Haën. Al powder (−325 mesh, 99.7% purity) was supplied by Strem Chemicals and was routinely used in the experiments reported. Al flakes (1.0 mm particle size, 99.99% purity) were supplied by Aldrich and were used to analyze the formation of a passive oxide layer on Al surface. All reagents were used as received. Deionized water was used to prepare all the aqueous solutions. The different solutions tested in this study were freshly prepared before performing the hydrogen production experiments.

2.2. Apparatus, materials and measurements

The equipment used in the hydrogen generation experiments has been described in a previous work [15]. Reagents were added in a 250 cm^3 Pyrex glass reactor containing 75 cm^3 of the selected aqueous solution. The reactor was heated in a water bath to maintain a constant temperature of 348 K. The mass of aluminum powder added to the reactor was fixed at 0.2 g for each experiment. Using 0.2 g Al powder it is possible to produce 272 cm^3 H_2 under standard conditions, assuming 100% hydrogen generation efficiency. Hydrogen production reactions started when the aluminum powder came into contact with the aqueous solution. Hydrogen produced by the reactions emerged from the reactor through a silicone tube of 40 cm length and 8 mm internal diameter; it was passed through a water bath at room temperature in order to condense the water vapor, and was collected in an inverted burette filled with water. The quantity of hydrogen gas produced was measured (at 298 K and 1 atm) from the water level change in the burette. All the experiments were performed under the conditions above described unless otherwise stated.

2.3. Byproduct analysis

Solid byproducts of the hydrogen generation reactions were analyzed with X-ray diffraction (XRD) for crystalline species identification. For XRD analysis of the byproducts, the solid mixture remaining in the reactor was filtered using a vacuum pump and a funnel provided with a filter plate. Solids were dried in an oven at 75 °C under air for approximately 24 h to remove humidity. The XRD analysis was also performed in air.

3. Results and discussion

Experiments with aqueous solutions of different compositions were performed at the same initial pH in order to determine the effect of sodium aluminate versus sodium hydroxide on the hydrogen production rates and yields. The experimental conditions and results obtained from these experiments are reported in Table 1. It is important to note that pH is a key parameter to modify hydrogen production efficiency. In accordance with previous works [9,10,15], a pH increase in the working aqueous solution enhances hydrogen production rates and yields. When the pH, the temperature of aqueous solution, the particle size of Al powder and the quantity

Table 1
Experimental conditions and results obtained with different solution compositions.

Initial pH	Solution composition	Yield (%)	Maximum flow rate (cm^3 H_2 min^{-1})	Final pH	$t_{(50\%)}$[a] (min)	Final time (min)
12.0	NaOH 0.01 M	22	26	11.2	–	70
	$NaAlO_2$ 0.06 M	33	20	12.3	–	75
13.0	NaOH 0.1 M	100	204	12.6	0.7	2.6
	$NaAlO_2$ 2.0 M	100	337	13.0	0.4	1.7

[a] Time when H_2 production achieved a yield value of 50%.

of added Al are fixed, the hydrogen production efficiency is only affected by the specific chemical composition of the aqueous solution used in each experiment. So, the results reported in Table 1 reveal that it is possible to enhance hydrogen evolution efficiency using $NaAlO_2$ instead of NaOH, obtaining better rates or yields at the same pH. Maximum flow rates were determined by maximum slope of hydrogen generation curves (see Fig. 1). A comparison of maximum flow rates, yields and times when 50% and 100% yield values are achieved showed that sodium aluminate improved hydrogen production efficiency with respect to sodium hydroxide. Concretely, the obtained yields at pH 12.0 are superior for the sodium aluminate experiment, and the observed hydrogen production rate at pH 13.0 for the sodium aluminate solution is more than 60% higher.

Hydrogen production rates and yields are affected by $NaAlO_2$ concentration, Al mass and temperature of the aqueous solution. The effects of these parameters on hydrogen production using sodium aluminate are described in the following sections in order to get a deeper insight into the present process.

3.1. Reproducibility of hydrogen generation in $NaAlO_2$

When using Al powder to generate hydrogen for power sources such as fuel cells, it is essential to control the rate and yield of hydrogen evolution from Al corrosion. In order to evaluate the reproducibility of hydrogen generation using sodium aluminate aqueous solutions, three experiments were performed under the same conditions. Typical hydrogen production curves (volume of H_2 produced versus time) are shown in Fig. 1 for these experiments in 0.49 M $NaAlO_2$ solution. As can be observed, after a short induction period (less than 15 s), hydrogen production rate is quite high at the first stages of the experiment, but it decreases as aluminum is being consumed. No significant differences are observed between curves. The average value of the maximum hydrogen flow rate was 160 H_2 cm^3 min^{-1} with an associated standard deviation of 4 H_2 cm^3 min^{-1}. The obtained mean yield was 77.0% (measured at 10 min) and its associated standard deviation was 0.2%. The small variations found between the three replicates, carried out under the same conditions confirmed that the present hydrogen generation measurements were reproducible.

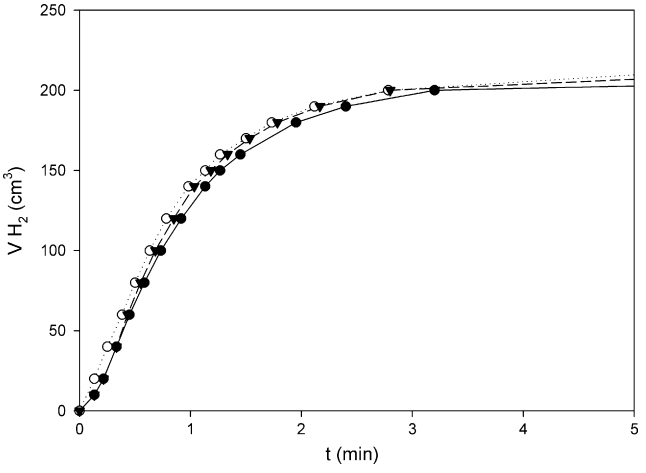

Fig. 1. Hydrogen generation curves obtained using an aqueous solution of $NaAlO_2$ 0.49 M at 348 K with 0.2 g Al powder. These three experiments were carried out under the same conditions.

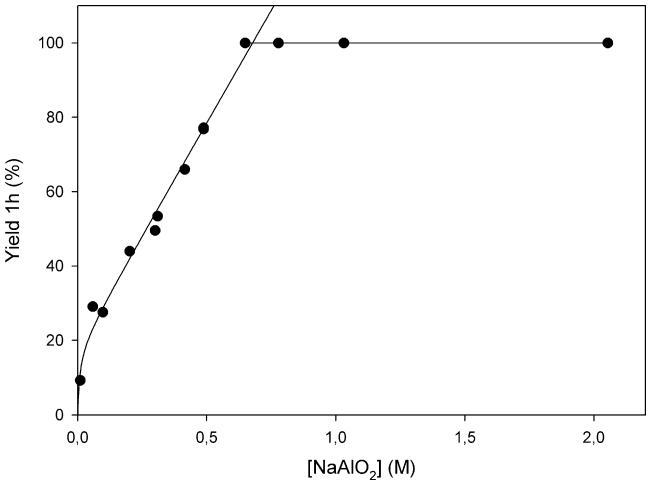

Fig. 2. Effect of $NaAlO_2$ concentration on H_2 production yield after 1 h of reaction.

3.2. Effect of sodium aluminate concentration

A systematic study was performed in order to determine the effect of $NaAlO_2$ concentration on hydrogen production efficiency. So, a series of experiments were carried out covering a range of concentrations between 0.01 and 2.05 M. The effects of $NaAlO_2$ concentration on hydrogen production yields and rates are shown in Figs. 2 and 3, respectively. An increase of $NaAlO_2$ concentration caused a raise in yields, reaching 100% within 1 h of reaction for concentrations equal or higher than 0.65 M, as can be observed in Fig. 2. Concerning maximum rates, the rate of H_2 evolution is faster

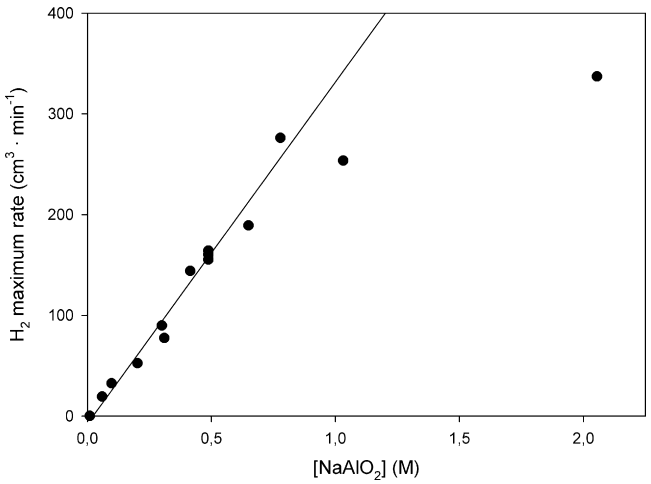

Fig. 3. Effect of $NaAlO_2$ concentration on maximum rate of H_2 generation.

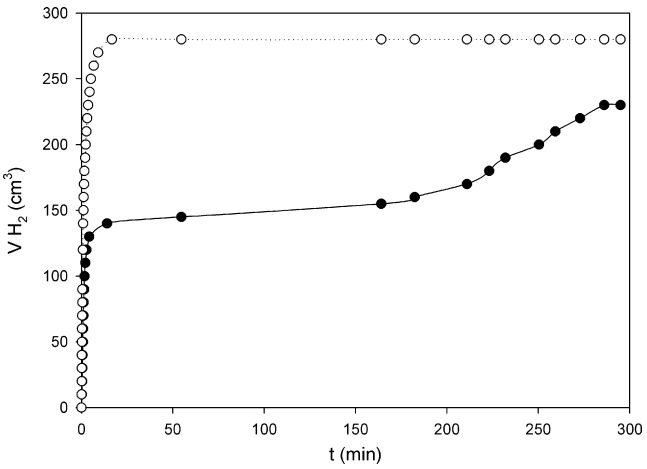

Fig. 4. Comparison of hydrogen evolution curves obtained for 0.2 g Al powder in $NaAlO_2$ 0.31 M (–●–) and $NaAlO_2$ 0.65 M (–○–) at 348 K.

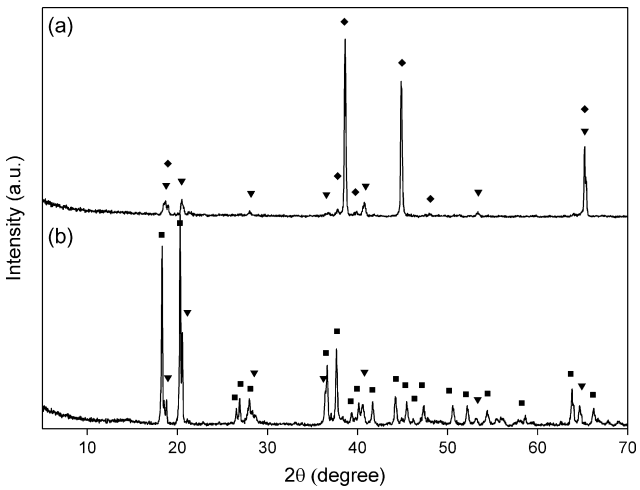

Fig. 5. XRD patterns of passivated surface of Al flakes (a) and solid byproduct using Al powder in $NaAlO_2$ solutions (b). Identification of diffracted peaks confirmed the presence of nordstrandite (♦) ($Al_2O_3{\cdot}3H_2O$), bayerite (▼) ($Al(OH)_3$) and gibbsite (■) ($Al(OH)_3$).

at higher $NaAlO_2$ concentration. In Fig. 3, a lineal relationship can be observed between maximum rates and $NaAlO_2$ concentration, confirming a first order H_2 production reaction at concentrations below 0.75 M. In contrast with the report of Aleksandrov et al. [22], an augment of aluminate ions in the aqueous solution enhanced hydrogen liberation.

Aluminum passivation and reactivation after some hours were observed in experiments performed at concentrations of $NaAlO_2$ between 0.10 and 0.31 M (see Fig. 4). This behavior can be attributed to the formation of an $Al(OH)_3$ layer on aluminum surface, which trapped water molecules that continued reacting with the metal to produce hydrogen [24] but at a much lower rate. The said hydrogen remained under the passive layer until the pressure of the gas was able to break it. Afterwards, the aqueous solution could contact the metal again, and a reactivation of the reaction was observed. For higher concentrations of aluminate (see upper curve in Fig. 4) this passivation interval was not found. Thus, our results indicate that the addition of aluminate anions in the aqueous solution has an effect on the passive film on the aluminum surface, reducing or preventing aluminum surface passivation (depending on reactants concentrations).

The formation of the mentioned passive oxide layer on Al surface was confirmed with an experiment in 0.1 M $NaAlO_2$ using 1.0 g Al flakes as raw material. An XRD analysis of passivated Al flakes, which were filtered and dried before reactivation took place, confirmed the formation of $Al(OH)_3$ (bayerite) and $Al_2O_3{\cdot}3H_2O$ (nordstrandite) thin layer on metallic Al surface (see Fig. 5). In contrast, an XRD analysis of final precipitate of the hydrogen generation reactions using Al powder in aqueous $NaAlO_2$ confirmed the formation of gibbsite and bayerite (different crystalline phases of $Al(OH)_3$).

In order to understand the kinetics of the hydrogen generation process, several kinetic models for solid–liquid heterogeneous systems were tested. These models usually depend on the degree of reaction (X), which is the ratio "reacted mass/initial mass". The obtained results were analyzed using two different shrinking core models [25], one controlled by a chemical step (4) and one controlled by mass transfer in the product layer (5). The equations describing these two models can be expressed as follows:

$$1-(1-X)^{1/3}=k_{ex}t \tag{4}$$

$$1-(2/3)X-(1-X)^{2/3}=k'_{ex}t \tag{5}$$

A satisfactory fitting of the model controlled by a chemical step (4) was observed during the first minutes of hydrogen evolution in all the experiments carried out with $NaAlO_2$ concentrations from 0.06 to 2.0 M. The model (4) was not valid when aluminum passivation prevailed. At that time the process presented a good fitting to the model controlled by mass transfer in the product layer (5) up to the end of reaction. The results are coherent with the formation of a passive hydroxide layer on the Al particles surface, which makes difficult the reagents diffusion from the aqueous solution towards the aluminum core. An example of fittings obtained is shown in Fig. 6 for $NaAlO_2$ 0.65 M.

From the matching of the model controlled by a chemical step it is also possible to calculate the apparent order of reaction n, since k_{ex} can be expressed as follows [25]:

$$k_{ex}=(bk_q\cdot C^n_{NaAlO_2})/(\rho_{Al}r_0) \tag{6}$$

The following relationship can be obtained by applying logarithms to Eq. (6):

$$\log k_{ex}=\log(bk_q/\rho_{Al}r_0)+n\log C_{NaAlO_2} \tag{7}$$

So, the order of reaction was determined by performing several experiments at constant temperature and r_0, covering a range of $NaAlO_2$ concentrations from 0.01 to 2.05 M, and plotting $\log k_{ex}$ versus $\log C_{NaAlO_2}$. A satisfactory fitting was obtained ($R^2=0.98$) with a slope value of 1.0, confirming a first order reaction before Al surface passivation takes control of the overall reaction rate. From the y-intercept, a value of the chemical reaction rate constant

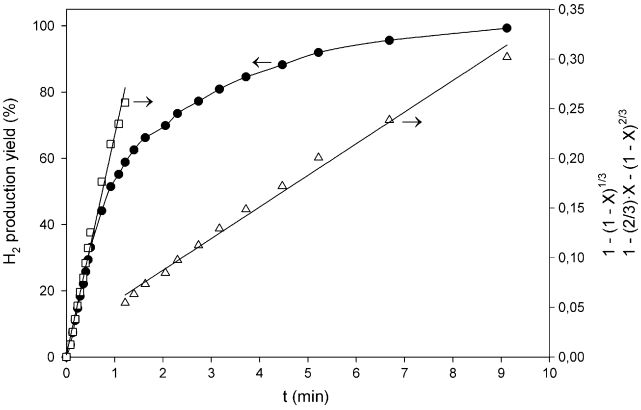

Fig. 6. Fitting of the experimental data obtained using $NaAlO_2$ 0.65 M by heterogeneous kinetic models controlled by a chemical step (□) and controlled mass transfer in the product layer (△).

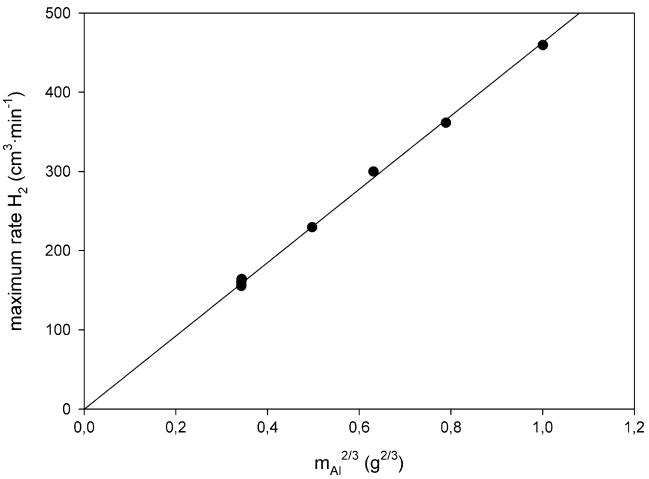

Fig. 7. Effect of Al quantity on maximum rate of H_2.production using $NaAlO_2$ 0.49 M.

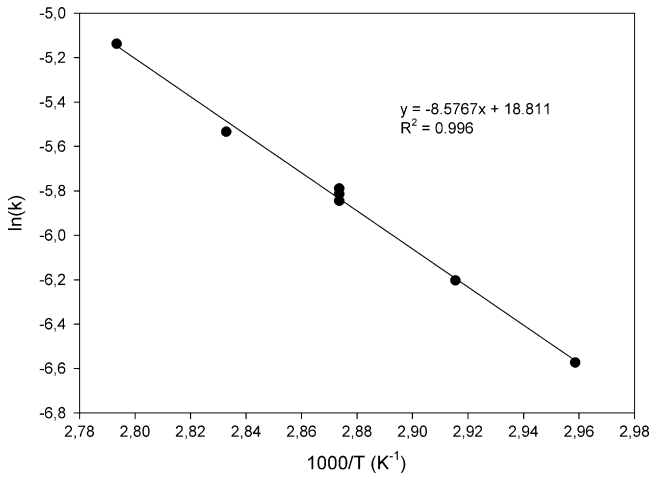

Fig. 8. Arrhenius plot of the rate constants using $NaAlO_2$ 0.49 M.

of $k_q = 0.010\,m\,s^{-1}$ at 348 K can be determined. The experiments using NaOH reported in Table 1 were also analyzed using Eqs. (4) and (5) in order to compare their kinetic behavior with the kinetics observed for $NaAlO_2$ solutions. A similar satisfactory fitting of the two selected kinetic models was found, confirming that the process is controlled by a chemical step until the passive thin layer is formed onto aluminum surface. Then, the model controlled by mass transfer in the product layer presented a good matching. Further determination of the order of reaction for NaOH solutions using Eq. (7) was also 1.0, confirming a first order reaction. Since reaction (2) is an equilibrium reaction, $NaAlO_2$ concentration and OH^- concentration are proportional and it can be concluded that systems with NaOH and $NaAlO_2$ solutions are first order reactions respect to OH^-, which suggests that the mechanism of Al corrosion in solutions of $NaAlO_2$ or NaOH could be the same.

3.3. Effect of Al mass

The relationship of the hydrogen release and the Al quantity was studied fixing the concentration of $NaAlO_2$ to 0.49 M and varying Al mass added in the reactor between 0.2 and 1.0 g. The results are shown in Fig. 7. As the Al quantity able to react with aqueous solution increased, the hydrolysis rate became faster. It was found that the maximum reaction rate followed a linear relationship on the initially added Al mass to the power of 2/3. This linear function (see Fig. 7) may be interesting in order to procure an appropriate hydrogen evolution rate in further applications. Similar results have been reported by Hu et al. [26] for Ni–Al alloys in NaOH solutions. Once again in contrast with results reported by Aleksandrov et al. [22] for Al powder, our experiments performed in NaOH solutions also showed that the maximum flow rate is a linear function of the initial Al mass to the power of 2/3.

3.4. Effect of temperature

The effect of temperature on the reaction rate was examined performing a series of tests at different temperatures. Prior to starting the experiments, $NaAlO_2$ 0.49 M solutions were initially heated to selected temperatures between 338 and 358 K. Once the temperature was equilibrated, the experiment was fulfilled by adding Al powder to the preheated $NaAlO_2$ solutions. As expected, the H_2 generation rate increases with the rise of temperature. To quantify this effect, we used the Arrhenius equation:

$$k = A\exp(-E_a/RT) \quad (8)$$

which gives the dependence of a rate constant (k) on the temperature (T) and the activation energy (E_a). By determining k from the maximum flow rates obtained at different temperatures and using Eq. (8), the activation energy of Al corrosion was calculated to be 71 kJ mol^{-1} from the plot of the reaction rate constant k against the reciprocal temperature, with a good linear fitting (see Fig. 8). An activation energy value higher than 40 kJ mol^{-1} indicates that the process is controlled by a chemical step rather than by mass transfer. This hypothesis was confirmed by the comparison of rates and yields of two hydrogen production experiments under the same conditions but with and without external agitation, which did not reveal significant variations.

Apparent activation energy was also calculated using the experimental rate constants k_{ex} obtained with Eq. (4) for the $NaAlO_2$ 0.49 M experiments at different temperatures from 338 to 358 K. A linear regression of $\ln(k_{ex})$ versus $1000/T$ was used to determine the activation energy value, and a good fitting was obtained. The apparent activation energy for the Al corrosion in $NaAlO_2$ 0.49 M solutions was determined to be ca. 79 kJ mol^{-1}, which is similar to the activation energy value obtained from the rate constants determined by maximum flow rates of H_2 production.

3.5. Mechanism of Al corrosion in $NaAlO_2$ and NaOH solutions

The previous literature on the reaction of hydrogen evolution activated by hydroxide ions has led to a considerable span on the activation energies obtained [11,22,27,29], although all of them point to a chemical reaction as rate determining step (except some time-dependent very low E_a reported in [29]), and also to different proposed mechanisms [22,24,28–30]. It is noteworthy that our experimental value of activation energy (71 kJ mol^{-1}) is concordant with the result of 68.4 kJ mol^{-1} obtained by Hiraki et al. [11] using NaOH 0.5 M. This similar activation energy points again to a similar mechanism of Al corrosion in the presence of $NaAlO_2$ or NaOH. The possibility of a unified mechanism is tempting, specially taking into account that the species present in the media, after the reaction has begun, are the same in both cases.

According to the results so far described, the following Al corrosion mechanistic scheme is proposed (except when the reaction is controlled by mass transfer in the product layer). The first stages of the reaction of aluminum in aqueous solutions would be carried out through three different reactions ((9–11)):

$$Al_2O_3 + 3H_2O \rightarrow 2Al(OH)_3 \quad (9)$$

$$Al(OH)_3 + OH^- \leftrightarrows Al(OH)_4^- \quad (10)$$

$$Al + 3H_2O \rightarrow Al(OH)_3 + 3/2H_2 \quad (11)$$

In principle, the maximum flow rate should occur at the beginning of the reaction since the Al quantity is the highest. However, the maximum rate was delayed for a short induction period because both the previous hydration of the surface oxide film on Al (reaction (9) [31]) and the dissolution of the $Al(OH)_3$ so formed, through step (10), are needed in order to expose the metal surface directly to water. Step (10) is an equilibrium reaction which appears to determine the reaction order and the reaction rate. The process is order 1 with respect to aluminate in the range of concentrations above quoted, and therefore with respect to the OH^- concentration, since both of them are proportional according to the equilibrium constant for step (10) ($K = 10^{1,5}$ [32]). The dependence of the hydrogen evolution rate on the amount of Al added can be also understood since its surface is recovered with $Al(OH)_3$, which should be removed by reaction (10) in order to uncover the bare Al surface, not only to initiate hydrogen evolution but along all the process.

When $NaAlO_2$ aqueous solutions are used, several aluminate species are initially present in the solution [23], including polymeric aluminate ions that can act as nuclei for $Al(OH)_3$ crystallization, thus competing with the $Al(OH)_3$ precipitation process on Al surface. In connection with this, let us retain that gibbsite and bayerite were found in the final precipitate while nordstrandite ($Al_2O_3{\cdot}3H_2O$, probably the initial product of alumina hydration) was only found on the Al surface for an unfinished experiment, suggesting that the final product grows on those nuclei. The equilibrium (10) allows an efficient transfer of at least part of the new aluminum hydroxide produced on the Al surface to the cited nuclei. This process allows to understand the depassivating effect of aluminate described in Section 3.2, thus facilitating reaction (11) between exposed Al and water and improving rates and yields with respect to experiments using only NaOH at the same initial pH.

Notice also that the final pH of the reactions in the aluminate solutions is higher than those in NaOH solutions (see Table 1). This fact can be due to the effect of aluminate as hydroxide supplier, again through the key equilibrium (10). Naturally, the more aqueous OH^- present, the faster reaction (10) is and, therefore, the faster the whole process should be.

Under our experimental conditions, the stage (11) should be a relatively fast and thermodynamically favored reaction ($\Delta G = -445\ kJ\ mol^{-1}$ of H_2) where hydrogen is produced. This reaction would proceed presumably through three consecutive elemental steps involving a water molecule and a hydrogen atom on each of them. The hydrogen atoms so formed would recombine very quickly to form H_2. This is, to the best of our knowledge, the simplest mechanism that allows to explain all the data reported so far (except the above-mentioned results in [22] and [29]), both in NaOH and $NaAlO_2$ solutions.

4. Conclusions

In this work, the kinetic and mechanistic features of hydrogen generation from Al corrosion in sodium aluminate solutions have been investigated. From the obtained results, the suitability of Al to produce hydrogen from aqueous solutions of $NaAlO_2$ has been demonstrated. High rates and low reaction times of aluminum corrosion in sodium aluminate aqueous solutions have revealed a promising system to obtain hydrogen for fuel cell applications. This process could abate production costs relative to processes based on hydrolysis of chemical hydrides as raw materials for *in situ* hydrogen generation. Concretely, some of the reported results obtained at different $NaAlO_2$ concentrations are potentially applicable in hydrogen supply devices for fuel cell applications. It has been shown how hydrogen production rate can be regulated varying experimental parameters such as the concentration of $NaAlO_2$, the temperature or the aluminum mass available. Two shrinking core kinetic models – Eqs. (4) and (5) – have been shown to fit the time-evolution of hydrogen release at two different stages of the process, both for NaOH and $NaAlO_2$ solutions. A mechanism – reactions (9–11) – unifying the behavior of Al corrosion in NaOH and $NaAlO_2$ solutions is proposed. The minor Al surface passivation observed in the presence of aluminate ions in the aqueous solution could be attributed to the rate-determining equilibrium reaction (10), which allows the efficient transfer of the new aluminum hydroxide produced to crystallization nuclei already present in the initial solution.

Acknowledgements

The authors express their gratitude to Air Products for financial support. Special thanks are given to Tim Golden for his helpful comments. J. Macanás thanks the support of Dept. d'Educació i Universitats de la Generalitat de Catalunya for a postdoctoral grant.

References

[1] P. Hoffmann, Tomorrow's Energy: Hydrogen, Fuel Cells, and the Prospects for a Cleaner Planet, first ed., MIT Press, USA, 2002, pp. 141–160.
[2] L. Soler, J. Macanás, M. Muñoz, J. Casado, Int. J. Hydrogen Energy 31 (2006) 129–139.
[3] M. Granovskii, I. Dincer, M.A. Rosen, J. Power Sources 167 (2007) 461–471.
[4] U. Eberle, G. Arnold, R. von Helmolt, J. Power Sources 154 (2006) 456–460.
[5] J.H. Wee, J. Power Sources 155 (2006) 329–339.
[6] H.Z. Wang, D.Y.C. Leung, M.K.H. Leung, M. Ni, Renew. Sustain. Energy Rev. (2008), doi:10.1016/j.rser.2008.02.009.
[7] S.C. Amendola, M. Binder, M.T. Kelly, P.J. Petillo, S.L. Sharp-Goldman, in: C.E. Grégorie Padró, F. Lau (Eds.), Advances in Hydrogen Energy, Kluwer Academic Publishers, New York, 2002, pp. 69–86.
[8] London Metal Exchange, the world centre for non-ferrous metals trading (data of consultation: 08/09/2008): http://www.lme.co.uk/aluminium.asp.
[9] D. Belitskus, J. Electrochem. Soc. 117 (1970) 1097–1099.
[10] D. Stockburger, J.H. Stannard, B.M.L. Rao, W. Kobasz, C.D. Tuck, in: A. Corrigan, S. Srinivasan (Eds.), Hydrogen Storage Materials, Batteries, and Electrochemistry, Electrochemical Society, USA, 1991, pp. 431–444.
[11] T. Hiraki, M. Takeuchi, M. Hisa, T. Akiyama, Mater. Trans. 46 (2005) 1052–1057.
[12] E.R. Andersen, E.J. Andersen. US Patent No. 6,638,493 B2 (2003).
[13] Q. Li, N.J. Bjerrum, J. Power Sources 110 (2002) 1–10.
[14] S.S. Martinez, W.L. Benítes, A.A. Álvarez, P.J. Sebastián, Sol. Energy Mater. Sol. Cells 88 (2005) 237–243.
[15] L. Soler, J. Macanás, M. Muñoz, J. Casado, J. Power Sources 169 (2007) 144–149.
[16] US DOE, Basic Research Needs for the Hydrogen Economy, 2003. Available online at http://www.sc.doe.gov/bes/hydrogen.pdf.
[17] L. Soler, J. Macanás, M. Muñoz, J. Casado, Int. J. Hydrogen Energy 32 (2007) 4702–4710.
[18] W.R. Busler, in: H.F. Mark, D.F. Othmer, C.G. Overberger, G.T. Seaborg, M. Grayson, D. Eckroth (Eds.), Kirk-Othmer Enciclopedia of Chemical Technology, vol. 2, Third ed., Wiley-Interscience, New York, 1978, pp. 197–202.
[19] J. Li, C.A. Prestidge, J. Addai-Mensah, J. Chem. Eng. Data 45 (2000) 665–671.
[20] S.H. Ma, S.L. Zheng, H.B. Xu, Y. Zhang, Trans. Nonferrous Met. Soc. China 17 (2007) 853–857.
[21] P. Sipos, G. Hefter, P.M. May, Talanta 70 (2006) 761–765.
[22] Y.A. Aleksandrov, E.I. Tsyganova, A.L. Pisarev, Russ. J. Gen. Chem. 73 (2003) 689–694.
[23] A. Buvári-Barcza, M. Rózsahegyi, L. Barcza, J. Mater. Chem. 8 (1998) 451–455.
[24] K. Ishii, R. Ozaki, K. Kaneko, H. Fukushima, M. Masuda, Corros. Sci. 49 (2007) 2581–2601.
[25] J. Viñals, in: A. Ballester (Ed.), Metalurgia Extractiva, Editorial Síntesis, Madrid, 2000, pp. 170–198.
[26] H. Hu, M. Qiao, Y. Pei, K. Fan, H. Li, B. Zong, X. Zhang, Appl. Catal. A: Gen. 252 (2003) 173–183.
[27] A.Z. Zhuk, A.E. Sheindlin, B.V. Kleymenov, E.I. Shkolnikov, M.Y. Lopatin, J. Power Sources 157 (2006) 921–926.
[28] Z.Y. Deng, J.M.F. Ferreira, J. Am. Ceram. Soc. 90 (2007) 1521–1526.
[29] A.I. Onuchukwu, A.I. Adamu, Mater. Chem. Phys. 25 (1990) 227–235.
[30] K.C. Emregül, A. Abbas Aksüt, Corros. Sci. 42 (2000) 2051–2067.
[31] X. Carrier, E. Marceau, J.F. Lambert, M. Che, J. Colloid Interface Sci. 308 (2007) 429–437.
[32] J. Heyrovský, J. Chem. Soc. Trans. 117 (1920) 1013–1025.